Technology for Improving Reliability of Oil-flooded Screw Compressors

Dr. Shoji YOSHIMURA Technical Development Department, Development Center, Machinery Business

Several issues exist with large oil-flooded screw compressors used for high-pressure. The large force, acting on their rotors, induces impact vibration between the male and female rotors, causing a large force acting on their bearings. In addition, the compressed gas directly contacts the lubricant, decreasing the oil viscosity. The present paper introduces new technologies, developed to resolve these issues.

Introduction

Oil-flooded screw compressors are widely used in industry because of their features including high efficiency, a small footprint and capacity control. Kobe Steel makes world-class oil-flooded screw compressors with maximum discharge pressures up to 10 MPaG and maximum rotor sizes up to about 500mm.

Screw rotors for large, high-pressure screw compressors are subject to large load and torque variations. Thus, the designing of such a compressor unit requires new technologies, and so does the designing of its peripheral equipment.

To ensure compressor reliability under such harsh operating conditions, Kobe Steel has developed several unique technologies and has delivered many compressors around the world. This paper introduces three typical technologies developed for improving the reliability of screw compressors.

1. Technical issues associated with reliability improvement

The following describes the main technical issues associated with improving the reliability of oil-flooded screw compressors.

- Abnormal vibration of screw rotors

Large pressure variations in the rotor groove increase the fluctuating torque acting on the rotors, causing the rotors to vibrate abnormally. Such abnormal vibrations shake the compressor units, increasing their noise, and can cause the rotors to be damaged.

- The prediction of bearing performance

The bearings of screw rotors are critical parts since they support the force caused by gas pressure and acting on the rotors. Thus, bearing analysis techniques are essential for developing compressors, making the prediction of bearing performance indispensable.

- Drop in lubricant viscosity

An oil-flooded compressor uses oil, poured into compressed gas, for cooling the gas and to improve the sealing between the engaged rotor grooves. The oil is collected by an oil recovery tank provided at the compressor outlet and is supplied to the bearings. Hydrocarbons, if contained in the compressed gas, can dissolve into the lubricating oil, decreasing the oil's viscosity, which deteriorates the bearing lubrication and can cause damage to the bearings. This necessitates a prediction technology for the reduction of lubricant viscosity.

Kobe Steel has overcome these technical challenges and succeeded in improving the reliability of screw compressors. The following outlines the technologies used for the improvement.

2. Analysis of screw rotor vibration [1~3)]

2.1 Rotor behavior

Fig. 1 shows the rotor profiles of a pair of engaging screw rotors. The arrows indicate the respective directions of rotation. The male rotor drives the female rotor and the rotors contact each other on their driving sides. For rotors in abnormal vibration, however, the screw rotors make contact on both their driving sides and trailing sides, resulting in a motion as depicted in **Fig. 2**. In the figure, the vertical axis (x) is the actual rotor clearance, while the horizontal axis represents time. The screw rotors have a designed clearance, δ, and $x = 0$ indicates a contact on the driving side, while $x = \delta$ indicates a contact on the trailing side. In other words, the vibration is caused

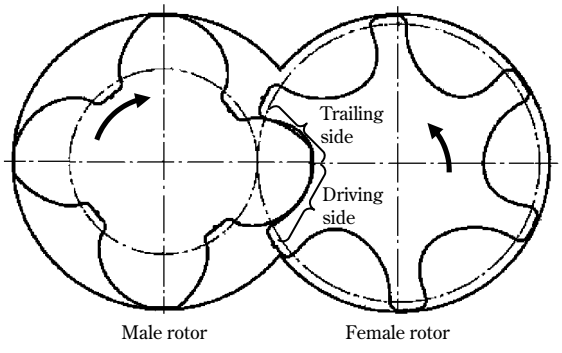

Fig. 1 Screw rotor profile

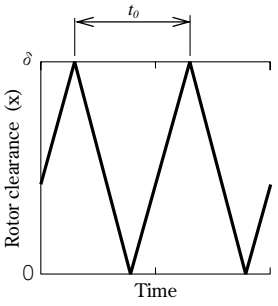

Fig. 2 Motion of rotors

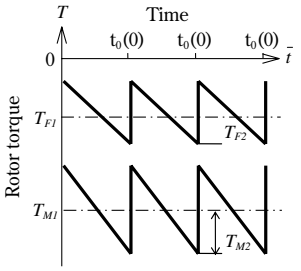

Fig. 3 Rotor torque

by periodic impacts on the driving side and trailing side, in which alternating collisions occur at a frequency of t_0.

The following summarizes the analysis of rotor behavior that causes impact vibration in a periodic manner as shown in Fig. 2.

2.2 Rotor motion equation

Fluctuating torque acts on the screw rotors as shown in **Fig. 3**, in which the horizontal axis represents time, $\bar{t}$. The time $\bar{t}=0$ is a time point at which the torque changes discontinuously, and t_0 represents the variation period of the torque. The time $\bar{t}=t_0$ ($t_0(0)$ in the figure) indicates the origin $\bar{t}=0$ of the next variation period of the torque. The torques acting on the female rotor and the male rotor are given by the following equations respectively:

$$T_F=T_{F1}+T_{F2}(1-2\bar{t}/t_0) \quad (0\le \bar{t}/t_0) \quad \cdots\cdots(1)$$

$$T_M=T_{M1}+T_{M2}(1-2\bar{t}/t_0) \quad (0\le \bar{t}/t_0) \quad \cdots\cdots(2)$$

The following describes the rotor behavior with the torques acting on the female and male rotors respectively, as shown in Fig. 3. By omitting negligible terms, the rotor motion equation is given as follows:

$$\frac{d^2x_F}{dt^2}=f_1+f_2(1-2t) \quad \cdots\cdots(3)$$

$$\mu\frac{d^2x_M}{dt^2}=-f_1+f_3(1-2t) \quad \cdots\cdots(4)$$

The respective variables and parameters are dimensionless quantities expressed as follows:

$t=\bar{t}/t_0$ $\quad x_F=\theta_F/\xi$

$x_M=\theta_M/\xi$ $\quad \mu=I_M/I_F/(N_M/N_F)^2$

$f_1=t_0^2T_{F1}/I_F/(N_M/N_F)/\xi$ $\quad f_2=t_0^2T_{F2}/I_F/(N_M/N_F)/\xi$

$f_3=t_0^2T_{M2}/I_F/(N_M/N_F)^2/\xi$

wherein

I_M and I_F are the inertia moments of the male and female rotors respectively;

θ_M and θ_F are the rotation angles of the male and female rotors respectively; and

N_M and N_F are the number of teeth of the male and female rotors respectively.

The angle ζ is the rotation angle of the male rotor corresponding to the rotor clearance. Here, the rotors are assumed to collide against each other with a coefficient of restitution R.

Examples of periodic vibration, caused by impact between the rotors, are shown in **Fig. 4** (a) and (b). The horizontal axis represents time, and one tick corresponds to one period of external force. The vertical axis represents rotor position. The periodical vibration waveform is expressed as vibration (J, K, L, M). Here, J, K, L and M are either zero or a positive integer respectively having the following meaning. It is to be noted that the number of branches described below represents the number of different types of vibration waveforms.

J is the external force periodic number;

K is the number of times the tooth flanks impact on the driving side;

L is the number of times the tooth flanks impact on the trailing side; and

M is the number of branches for the periodic vibration.

The vibration that can lead to abnormal vibration is represented in Fig.4 (a), in which tooth flanks impact on the trailing side periodically. In the case of the vibration shown in Fig.4 (b), the tooth flanks do not make contact on the trailing side; however, it causes abnormal sound.

2.3 Stable regions for periodic vibration

Periodic vibrations are calculated from the vibration waveforms shown in Fig. 4. The stable regions for the periodic vibrations are determined by a characteristic equation. The stable region for (J, 1, 0, 1) vibration is analytically calculated as follows:

$$0<\frac{f_2}{f_1}(1-2t_p)\left(1-\frac{f_3}{\mu f_2}\right)<\frac{1+\mu}{\mu}\left\{1+\left(\frac{1-R}{1+R}\right)^2\right\} \quad \cdots(5)$$

wherein

$$t_p=\frac{1}{2}\left\{1\pm\sqrt{\frac{1}{3}+2J\frac{(1+\mu)f_1}{f_3-\mu f_2}\left(1-\frac{2R}{1+R}\right)}\right\} \quad \cdots\cdots(6)$$

The stable region for (1, K, 1, M) vibration can not

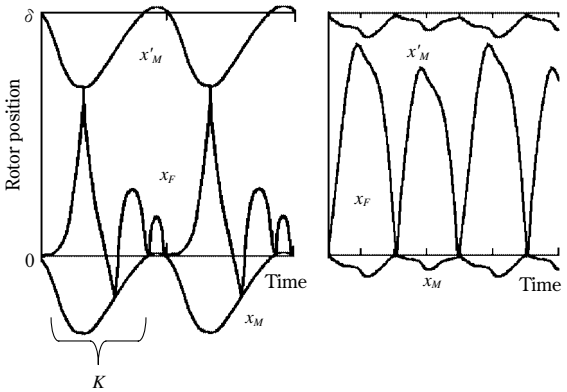

(a) (1, K, 1, 1) Vibration (b) (2, 1, 0, 2) Vibration

Fig. 4 Periodic vibration

be obtained analytically and is determined by numerical calculation.

Fig. 5 shows the stable regions for a conventional rotor profile calculated from its periodic vibration. The areas surrounded by solid lines are stable regions for impact vibration caused by the tooth flanks impacting each other as shown in Fig. 4 (a). The area surrounded by a dashed-dotted line is the stable region for the impact vibration caused by the tooth flanks impacting on their driving sides only as shown in Fig. 4 (b). The horizontal axis represents f_2. The vertical axis is f_2/f_1 which corresponds to the rotor torque and is determined by the pressure condition of the compressors. The parameters f_2 and f_2/f_1 of the conventional rotor profile correspond to the solid circle (●) which falls in a stable region of periodic vibration. Thus the conventional rotor profile can exhibit abnormal vibration.

A rotor profile has been developed which prevents abnormal vibration. **Fig. 6** shows the stable region derived from the periodic vibration of the newly developed rotor profile. The newly developed rotor profile has a small stable region and its f_2 and f_2/f_1 fall on the black circle which is located away from the stable region, eliminating the possibility of abnormal vibration.

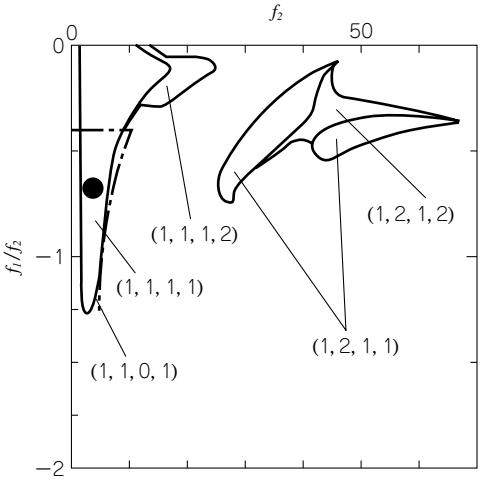

Fig. 5 Stable region of periodic vibration for conventional profile

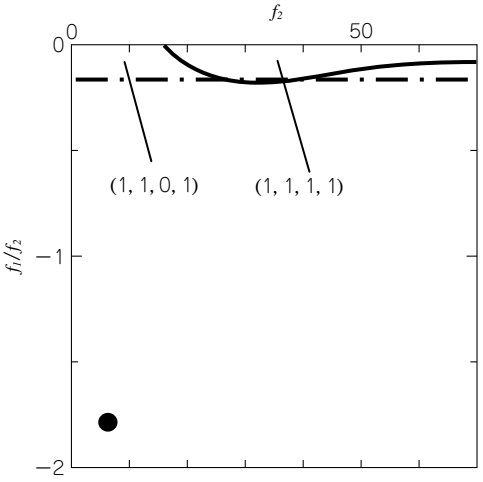

Fig. 6 Stable region of periodic vibration for new profile

3. Bearing analysis technique

3.1 Bearing load

Gas pressure acts on a bearing via a screw rotor. The bearing loads, radial load (F_R) and thrust load (F_S), are approximated by the following equations respectively:

$$F_R = \alpha DL(P_D - P_S) \quad \cdots\cdots(7)$$

$$F_S = \beta D^2(P_D - P_S) \quad \cdots\cdots(8)$$

wherein D is rotor diameter, L is rotor length, P_D is discharge pressure and P_S is suction pressure. The α and β are coefficients determined from rotor profiles.

The bearing area depends on the bearing diameter, i.e., on the rotor diameter D. It should be noted that, as expressed by the equations (7), (8), the bearing load can increase to a level exceeding the allowable pressure and damage the bearing, regardless of the bearing size. Thus, it is essential to clarify the bearing characteristics.

3.2 Primitive equation for slide bearings

The bearing characteristics of a slide bearing are analyzed for bearing development. A slide bearing forms an oil film through the relative motion between the shaft and bearing surface. This oil film supports the bearing load. **Fig. 7** shows a schematic planer bearing having a varying clearance, in which the horizontal axis is x, and the vertical axis corresponds to the bearing clearance $h(x)$. The distribution pressure in the oil film is expressed as $p(x, z)$, in which z is the coordinate position in the thickness direction of Fig. 7. Assuming a bearing having a width of B, with the pressures at both ends of the bearing being at atmospheric pressure p_0, the pressure boundary condition is expressed by the following:

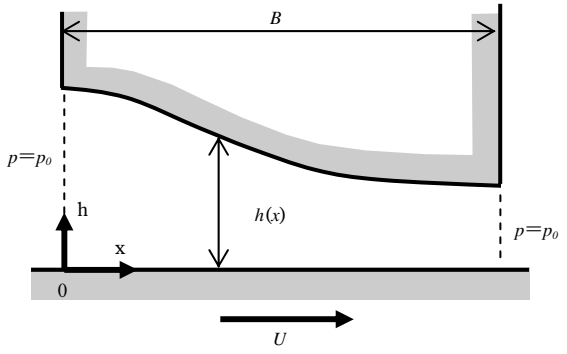

Fig. 7 Oil film bearing

$$p(0, z)=p_0,\ p(B, z)=p_0 \quad \cdots\cdots(9)$$

When the bearing surface (the bottom portion of Fig. 7) moves at a velocity of U, the relation between $h(x)$ and $p(x, z)$ is derived from the Reynolds equation as follows:

$$\frac{\partial}{\partial x}\left(\frac{h^3}{\eta}\frac{\partial p}{\partial x}\right)+\frac{\partial}{\partial z}\left(\frac{h^3}{\eta}\frac{\partial p}{\partial x}\right)=6U\frac{\partial h}{\partial x} \quad \cdots\cdots(10)$$

wherein η is the viscosity of the oil. Since the oil viscosity is significantly affected by temperature, the temperature distribution in the oil film should also be calculated. The temperature of an oil film is calculated from the heat generated by the shear and the transfer of oil, thermal conductance and the balance of heat transferred between the shaft and bearing.

The amount of heat Q_1 generated per unit area by shear is given by

$$Q_1=U\left(-\frac{h}{2}\frac{\partial p}{\partial x}+\frac{\eta U}{h}\right) \quad \cdots\cdots(11).$$

While the amount of heat transferred Q_2, caused by the transfer and thermal conductance of an oil film, having a temperature of T is given by

$$Q_2=\lambda\left(\frac{\partial^2 T}{\partial x^2}+\frac{\partial^2 T}{\partial z^2}\right)-C\gamma\left(u\frac{\partial T}{\partial x}+w\frac{\partial T}{\partial z}\right) \quad \cdots\cdots(12),$$

the amount of heat, Q_3, transferred to the shaft and bearing, is expressed as follows:

$$Q_3=\alpha_A(T-T_A)+\alpha_B(T-T_B) \quad \cdots\cdots(13)$$

wherein

λ is the thermal conductivity of the oil;

C is the specific heat of the oil;

γ is the specific gravity of the oil;

α_A is the heat-transfer coefficient between the shaft and oil film;

α_B is the heat-transfer coefficient between the bearing and oil film;

u, w are the rate of the flow oil in the directions of x, z respectively; and

T_A, T_B are the surface temperatures of the shaft and bearing respectively.

The following equation holds from the heat balance.

$$Q_1=Q_2+Q_3 \quad \cdots\cdots(14)$$

Furthermore, the relation between the oil temperature and viscosity is expressed as follows:

$$\eta=10^{10^{|A-B\log(T)|}} \quad \cdots\cdots(15)$$

wherein A and B are constants.

The oil pressure generated, $p(x, z)$, and oil film temperature are determined by solving the equations (10) - (15). Integrating $p(x, z)$ for the bearing surface yields the oil film force (i.e., bearing force). This force balances with the bearing load.

3.3 Simulation program for bearing characteristics

A simulation program for bearing characteristics has been developed, using the difference method, based on the equations (10) - (15) described in section 3.2. Equations (10) - (15) calculate the bearing force for predetermined bearing clearances. In reality, however, the bearing load is predetermined, and the bearing clearance is calculated iteratively, such that the predetermined bearing load matches the bearing force.

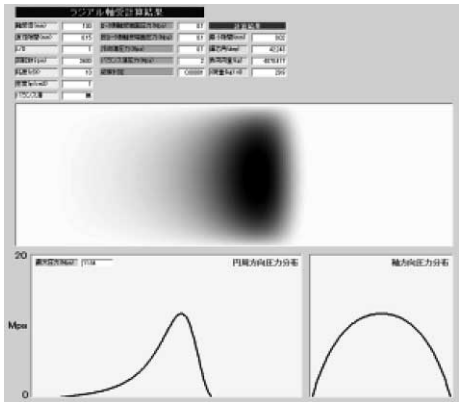

Fig. 8 Bearing simulation

Fig. 8 shows a sample result obtained by the simulation program for bearing characteristics. The diagram in the middle shows the pressure distribution calculated by the equation (10), with the horizontal axis indicating the circumferential direction and the vertical axis indicating the shaft direction of the bearing. In this diagram, a darker area depicts the part in which the oil pressure is higher. The graph at the lower left shows the oil pressure along the circumferential direction of the bearing, while the graph at the lower right shows the oil pressure along the shaft direction. The calculation yields the minimum oil-film thickness and bearing temperature; the values provide indication as to whether or not sufficient bearing clearance is secured. It should be noted that the heat-transfer coefficients are determined experimentally due to the difficulty of determining them theoretically.

4. Technique for predicting oil viscosity

4.1 Dissolution of gas into lubricant

Fig. 9 is a flow chart of fluid in an oil-flooded screw compressor consisting of a compression chamber, bearing and oil cooler. In this compressor, the oil, poured into the compression chamber and the bearing, is mixed with gas. An oil recovery tank at the compressor outlet separates the gas and oil. The separated oil goes through the cooler and is poured into the compression chamber and bearings again.

In many cases, gas contains a hydrocarbon (CmHn), which decreases oil viscosity during the

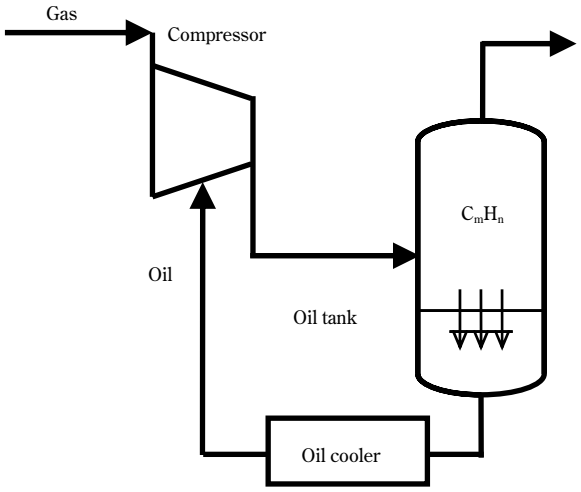

Fig. 9 Flow diagram of an oil-flooded screw compressor

compression process. Decreased oil viscosity may cause insufficient lubrication of the bearings. Thus, it is important to predict the decrease in oil viscosity and select more viscous oil.

4.2 Equation for predicting oil viscosity

Provided that the content of CmHn in the incoming gas is x% and the discharge pressure is P_D, the partial pressure of CmHn at the compressor outlet is expressed as follows:

$$P_X = \frac{x}{100} P_D \quad \cdots\cdots(16)$$

The amount G_X of CmHn dissolved into the oil in the oil recovery tank is calculated by ROULT's law as follows:

$$P_X = P_C \frac{G_X/M_C}{G_X/M_C + G_0/M_0} \quad \cdots\cdots(17)$$

wherein

P_C is the saturation vapor pressure of CmHn at the discharge temperature;

G_X is the mass of CmHn;

M_C is the molecular weight of CmHn;

G_0 is the mass of oil; and

M_0 is the molecular weight of the oil.

After passing the compressor, the oil is cooled and poured into the compressor again. Here, the viscosity at a feed temperature is calculated for the oil having a mass of G_0, with a mass, G_X, of CmHn dissolved in the oil. Provided that the viscosity of the oil at the feed temperature is μ_0 and the viscosity of CmHn is μ_c, the viscosity of the mixture, μ, is expressed as follows:

$$\log \mu = K_0 \log \mu_0 + K_c \log \mu_c \quad \cdots\cdots(18)$$

wherein

$$K_0 = \frac{W_0/A}{W_0/A + W_C/M_C}$$

$$K_C = \frac{W_C/M_C}{W_0/A + W_C/M_C}$$

$$W_0 = \frac{G_0}{G_0 + G_X}$$

$$W_C = \frac{G_X}{G_0 + G_X}$$

in which A is the constant determined by the type of lubricant. The equation (18) is the prediction equation for one component gas, CmHn. In reality, however, more than one component may dissolve into the gas. In addition, the decrease in viscosity depends on the type of CmHn. Thus, the comprehensive equation covering all cases becomes rather complex and is omitted here.

4.3 Verification of forecast equation by elemental experiment

The equations (16) and (17) are valid only for ideal conditions. The behaviors in reality do not follow the theoretical formula in many cases. In particular, CmHn has a molecular structure similar to that of oil and strongly interacts with oil. Thus a correction term must be calculated experimentally. **Fig. 10** compares the vapor pressures, theoretically predicted and experimentally measured, of CmHn mixed with mineral oil. The prediction well matches the experiment for benzene; however, there are slight discrepancies for toluene and xylene. Similar discrepancies are observed for other substances and, for that reason, the equation (17) must be used with corrections.

Fig. 11 compares the viscosities, theoretically predicted and experimentally measured, for a mixture of benzene and mineral oil. The value, A, of equation (18) is obtained by experiment and, if used

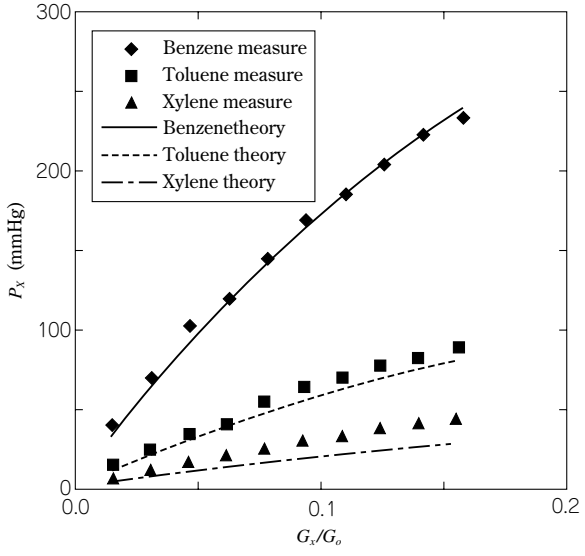

Fig.10 Vapor pressure of a mixture with oil and HmCn

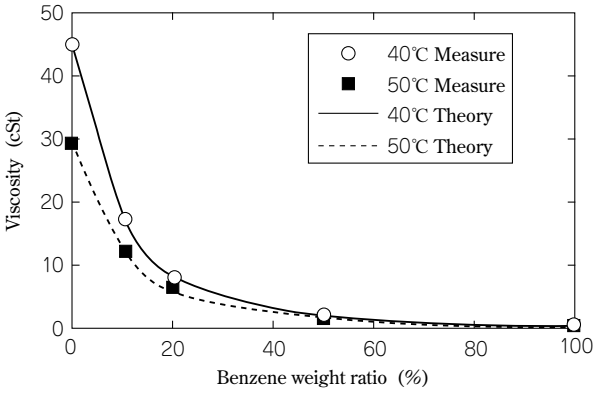

Fig.11 Viscosity of the mixture of oil and benzene

herein, results in a better match with the theoretical value.

Kobe Steel is now able to predict the oil viscosity, using theoretical formulae corrected by experimental data and is thus able to select the most appropriate types of oil.

Conclusion

The oil-flooded screw compressors of Kobe Steel have advanced features offered by carefully selected oil poured into compressed gas. The oil cools the gas and seals the compressor by forming a film. In addition, the compressors fully exploit their unique capacity control capability, offering advantages superior to those of other compressors. In the past, the oil caused various problems; however, Kobe Steel has successfully solved these problems and has developed compressors of larger sizes and with a high pressure capacities, which are unprecedented anywhere else in the world. Kobe Steel will strive to develop compressors for new applications based on those technologies.

References

1) S. Yoshimura : *Impact Vibration of Screw Compressor Rotor (In the Case That Vibration Occurs at the Driving Side), Transaction of JSME*, 1995, Vol. 61, No.582, C, p.501.
2) S. Yoshimura : *Impact Vibration of Screw Compressor Rotor (In the Case That Vibration Occurs at Both the Driving and Trailing Side), Transaction of JSME*, 1995, Vol. 61, No.586, C, p.2216.
3) S. Yoshimura : *Impact Vibration of Screw Compressor Rotor (3rd Report, Analysis in consideration of Inertia of both rotors), Transaction of JSME*, 1998, Vol.64, No.617, C, p.15.